

# Effective oscillator strength distributions of spherically symmetric atoms for calculating polarizabilities and long-range atom-atom interactions

Jun Jiang<sup>a,b,\*</sup>, J. Mitroy<sup>b</sup>, Yongjun Cheng<sup>b,c</sup>, M. W. J. Bromley<sup>d</sup>

<sup>a</sup>*Key Laboratory of Atomic and Molecular Physics and Functional Materials of Gansu Province, College of Physics and Electronic Engineering, Northwest Normal University, Lanzhou 730070, P. R. China*

<sup>b</sup>*School of Engineering, Charles Darwin University, Darwin, Northern Territory, 0909, Australia*

<sup>c</sup>*Academy of Fundamental and Interdisciplinary Science, Harbin Institute of Technology, Harbin 150080, P. R. China*

<sup>d</sup>*School of Mathematics and Physics, The University of Queensland, Brisbane, Queensland 4075, Australia*

## Abstract

Effective oscillator strength distributions are systematically generated and tabulated for the alkali atoms, the alkaline-earth atoms, the alkaline-earth ions, the rare gases and some miscellaneous atoms. These effective distributions are used to compute the dipole, quadrupole and octupole static polarizabilities, and are then applied to the calculation of the dynamic polarizabilities at imaginary frequencies. These polarizabilities can be used to determine the long-range  $C_6$ ,  $C_8$  and  $C_{10}$  atom-atom interactions for the dimers formed from any of these atoms and ions, and we present tables covering all of these combinations.

---

\*Corresponding author.

Email addresses: phyjiang@yeah.net (Jun Jiang), cyj83mail@gmail.com (Yongjun Cheng), brom@physics.uq.edu.au (M. W. J. Bromley)

## Contents

1.	Introduction . . . . .	3
2.	Definitions . . . . .	4
2.1.	Oscillator strength sum-rules . . . . .	4
2.2.	Casimir-Polder relations . . . . .	8
2.3.	Quadrature rules for Casimir-Polder integrations . . . . .	9
3.	Atomic Models . . . . .	9
3.1.	Hydrogen . . . . .	10
3.2.	Core oscillator strength distributions for multi-electron atoms . . . . .	10
3.3.	General comment for the alkali atoms and alkali-like ions . . . . .	11
3.4.	Lithium . . . . .	12
3.5.	Sodium . . . . .	13
3.6.	Potassium . . . . .	13
3.7.	Rubidium . . . . .	13
3.8.	Cesium . . . . .	13
3.9.	Copper and Silver . . . . .	13
3.10.	$\text{Be}^+$ . . . . .	13
3.11.	$\text{Mg}^+$ . . . . .	14
3.12.	$\text{Ca}^+$ . . . . .	14
3.13.	$\text{Sr}^+$ . . . . .	14
3.14.	$\text{Ba}^+$ . . . . .	14
3.15.	Beryllium . . . . .	14
3.16.	Magnesium . . . . .	15
3.17.	Calcium . . . . .	15
3.18.	Strontium . . . . .	15
3.19.	Barium . . . . .	15
3.20.	Helium( $1s^2$ ) . . . . .	16
3.21.	Neon, argon, krypton and xenon . . . . .	16
3.22.	$\text{He}(1s2s\ ^3S^e)$ . . . . .	16
3.23.	Overview . . . . .	17
4.	Dynamic polarizability and dispersion coefficient tabulations . . . . .	17
4.1.	Real frequencies . . . . .	17
4.2.	Imaginary frequencies . . . . .	17

4.3. Dispersion coefficients .....	18
4.4. Impact of finite precision tabulations .....	18
5. Conclusion .....	18
References .....	19
Explanation of Tables .....	24
Tables	
1. Multipole static polarizabilities and atom-wall dispersion parameter for all atoms and ions.	
See Page 24 for explanation of tables.....	26
2. The dipole, quadrupole and octupole effective oscillator strength distributions. See Page 24 for explanation of tables.....	27
3. The dipole, quadrupole and octupole dynamic polarizabilities (in a.u.) for all atoms and ions. See Page 25 for explanation of tables.....	33
4. Dispersion coefficients of $C_6$ , $C_8$ and $C_{10}$ . See Page 25 for explanation of tables. ....	41

## 1. Introduction

The long-range interaction between two spherically symmetric atoms can be written in the general form [1, 2, 3, 4]

$$V(R) \approx -\frac{C_6}{R^6} - \frac{C_8}{R^8} - \frac{C_{10}}{R^{10}} + \dots , \quad (1)$$

where the  $C_n$  parameters are the London/van der Waals dispersion coefficients. There are two complementary approaches to the computation of the dispersion coefficients. One approach uses oscillator strength sum-rules [5, 6], while the second utilizes Casimir-Polder relations and uses the dynamic polarizabilities computed at imaginary energies [7, 8]. These approaches can be regarded as complementary to each other.

The key to the first approach is to generate an oscillator strength distribution that incorporates excitations to bound excited states and to the continuum states. In practice, the oscillator strength distributions are best termed ‘effective’ oscillator strength distributions [9]. One might find that the lowest few excited states are accurately represented by the distribution, however the higher bound states and continuum states are approximated with a set of discrete effective oscillator strengths and energies. The oscillator strength distributions can be derived from *ab-initio* structure calculations

[10, 11, 12, 4], experimental information such as refractive indices, atomic transition rates and photo-ionization cross sections [5, 6], and sometimes both experimental and calculated oscillator strengths are used [12, 13].

The Casimir-Polder relation is reliant on being able to calculate the dipole and multipole dynamic polarizabilities at imaginary frequencies. One way to calculate a dynamic polarizability is to use oscillator strength sum-rules in conjunction with a previously determined oscillator strength distribution. An alternate approach is to directly compute the dynamic polarizability as part of a structure calculation [14, 15, 16]. The direct calculation of the dynamic polarizability is the preferred approach for structure calculations.

The present paper reports both effective oscillator strength distributions and dynamic polarizabilities for a number of spherically symmetric atoms and ions. The atoms presented are the noble gases, the alkali atoms and hydrogen, the singly-charged alkaline-earth ions and the alkaline earth atoms. The long-range atom-atom interaction coefficients  $C_6$ ,  $C_8$  and  $C_{10}$  are also presented for any dimer formed from these atoms and ions. A previous tabulation of dynamic polarizabilities for many of these atoms does exist [17]. This previous tabulation only gave the dynamic dipole polarizabilities, while the present tabulation extends this to the quadrupole and octupole polarizabilities that are needed in the evaluation of  $C_8$  and  $C_{10}$ . The  $C_8$  and  $C_{10}$  dispersion coefficients are typically included in analysis of diatomic spectra aimed at characterizing the inter-atomic potential curve [18, 19, 20]. At distances beyond the LeRoy radius [21, 22] the inter-atomic interaction is reasonably well described by an interaction consisting exclusively of the dispersion interaction with the  $C_6$ ,  $C_8$  and  $C_{10}$  terms [4, 23].

## 2. Definitions

### 2.1. Oscillator strength sum-rules

All of the polarization parameters that are reported were computed from their respective oscillator strength sum-rules with the dipole, quadrupole and octupole oscillator strengths  $f_{0i}^{(\ell)}$  from the ground state (with orbital and spin angular momentum equal zero) to the  $i$ th excited state defined [11, 4] as

$$f_{0i}^{(\ell)} = \frac{2|\langle\psi_0 \parallel r^\ell \mathbf{C}^\ell(\hat{\mathbf{r}}) \parallel \psi_i\rangle|^2 \epsilon_{0i}}{(2\ell+1)}. \quad (2)$$

In this expression  $\mathbf{C}^\ell$  is the spherical tensor of rank  $\ell$  while  $\epsilon_{0i}$  is the excitation energy of the transition. The sum-rule for the adiabatic multipole polarizability,  $\alpha^{(\ell)}$  [24, 4] is

$$\alpha^{(\ell)} = \sum_i \frac{f_{0i}^{(\ell)}}{(\epsilon_{0i})^2} . \quad (3)$$

One can also define other sum-rules [25, 26, 24] such as

$$S^{(\ell)}(-k) = \sum_i \frac{f_{0i}^{(\ell)}}{(\epsilon_{0i})^k} , \quad (4)$$

where the  $S^{(\ell)}(-2)$  are just the multipole polarizabilities. The Thomas-Reiche-Kuhn (TRK) sum-rule says that  $S^{(1)}(0)$  is equal to the number of electrons in the atom [27, 28, 29]. There also is the atom-wall dispersion parameter,  $C_3$  defined as [30, 31, 4]

$$C_3 = \frac{1}{8} \sum_i \frac{f_{0i}^{(1)}}{\epsilon_{0i}} = \frac{1}{8} S^{(1)}(-1) . \quad (5)$$

These sum-rules are a generalized sum which implicitly includes a sum of excitations to ( $E < 0$ ) bound states and an integration taking into account excitations to ( $E > 0$ ) continuum states. In the present work the sum-rule is explicitly discretized, which is a consequence of diagonalization in a finite-sized box due to the finite range of the chosen basis wave functions.

A similar application of the oscillator strengths is to determine the standard atom-atom adiabatic dispersion parameters. The dipole-dipole dispersion parameter between atoms A and B,  $C_6$  is [24, 32]

$$C_6^{\text{AB}} = \frac{3}{2} \sum_{ij} \frac{f_{A,0i}^{(1)} f_{B,0j}^{(1)}}{\epsilon_{A,0i} \epsilon_{B,0j} (\epsilon_{B,0j} + \epsilon_{B,0i})} , \quad (6)$$

the dipole-quadrupole dispersion parameter,  $C_8$  is [24, 32]

$$C_8 = \frac{15}{4} \sum_{ij} \frac{f_{A,0i}^{(1)} f_{B,0j}^{(2)}}{\epsilon_{A,0i} \epsilon_{B,0j} (\epsilon_{A,0i} + \epsilon_{B,0j})} + \frac{15}{4} \sum_{ij} \frac{f_{B,0i}^{(1)} f_{A,0j}^{(2)}}{\epsilon_{B,0i} \epsilon_{A,0j} (\epsilon_{B,0i} + \epsilon_{A,0j})} , \quad (7)$$

and the dispersion parameter,  $C_{10}$  is [24, 32]

$$\begin{aligned} C_{10} = & 7 \sum_{ij} \frac{f_{A,0i}^{(1)} f_{B,0j}^{(3)}}{\epsilon_{A,0i} \epsilon_{B,0j} (\epsilon_{A,0i} + \epsilon_{B,0j})} + 7 \sum_{ij} \frac{f_{A,0i}^{(3)} f_{B,0j}^{(1)}}{\epsilon_{A,0i} \epsilon_{B,0j} (\epsilon_{A,0i} + \epsilon_{B,0j})} \\ & + \frac{35}{2} \sum_{ij} \frac{f_{A,0i}^{(2)} f_{B,0j}^{(2)}}{\epsilon_{A,0i} \epsilon_{B,0j} (\epsilon_{A,0i} + \epsilon_{B,0j})} . \end{aligned} \quad (8)$$

In a large dimension atomic structure calculation the sum-rules defined in Eq. 4 are calculated as:

$$S^{(\ell)}(-k) = \sum_{c=1}^{N_c} \frac{f_c^{(\ell)}}{\epsilon_c^k} + \sum_{i=1}^N \frac{f_i^{(\ell)}}{\epsilon_i^k} \rightarrow \sum_{c=1}^{N_c} \frac{f_c^{(\ell)}}{\epsilon_c^k} + \sum_{r=1}^{N_{r'}} \frac{f_r^{(\ell)}}{\epsilon_r^k} + \sum_{r=N_{r'}}^{N_r} \frac{f_r^{(\ell)}}{\epsilon_r^k} + \sum_p \frac{f_p^{(\ell)}}{\epsilon_p^k} . \quad (9)$$

Here, the first sum (with  $f_c, \epsilon_c$ ) uses the core oscillator strength distribution for the number of core-electrons ( $N_c$ ) which is discussed later. The valence oscillator strength distribution from a calculation of size  $N$  can be logically broken up into the last three terms. Both the second and third sums (with  $f_r, \epsilon_r$ ) represent the excitations to real (physical,  $E < 0$ ) bound states. The second sum represents the contributions from the lowest, for example,  $N_{r'} = 4$  excited states which typically account for more than 95% of the sum-rule for dipole excitations, while the excitations to more highly excited bound states are incorporated in the third sum. The fourth term (with  $f_p, \epsilon_p$ ) contains the pseudo-oscillator strengths for excitations to ( $E > 0$ ) continuum states.

The multipole valence oscillator strength distributions typically contain  $N = 15 - 6000$  terms for each multipole. Distributions with more than 20 terms for a given multipole are too unwieldy for tabulation and easy computation. The solution to this problem is to construct an effective oscillator strength distribution ( $f_e, \epsilon_e$ ) [33, 9] in which a few effective oscillator strengths were adopted to represent the impact of the excitations to highly-excited bound states and continuum states, that is, of the third and fourth sums in Eq. 9. In the present work, the sum-rule involving the effective oscillator strength distributions is calculated as

$$S_e^{(\ell)}(-k) = \sum_{c=1}^{N_c} \frac{f_c^{(\ell)}}{\epsilon_c^k} + \sum_{r=1}^{N_{r'}} \frac{f_r^{(\ell)}}{\epsilon_r^k} + \sum_{e=1}^{N_e} \frac{f_e^{(\ell)}}{\epsilon_e^k}. \quad (10)$$

The effective oscillator strength distribution ( $f_e, \epsilon_e$ ) is solved by setting the new sum-rules  $S_e^{(\ell)}(-k)$  equal to the sum-rules  $S^{(\ell)}(-k)$  calculated from large dimension atomic structure calculations. For example, a new distribution with two effective transitions  $(f_{e1}, \epsilon_{e1}, f_{e2}, \epsilon_{e2})$  is the solution of the non-linear equations constituted of four sum-rules:

$$S^{(\ell)}(0) = \sum_{c=1}^{N_c} f_c + \sum_{r=1}^{N_{r'}} f_r + f_{e1} + f_{e2} \quad (11)$$

$$S^{(\ell)}(-1) = \sum_{c=1}^{N_c} \frac{f_c}{\epsilon_c} + \sum_{r=1}^{N_{r'}} \frac{f_r}{\epsilon_r} + \frac{f_{e1}}{\epsilon_{e1}} + \frac{f_{e2}}{\epsilon_{e2}} \quad (12)$$

$$S^{(\ell)}(-2) = \sum_{c=1}^{N_c} \frac{f_c}{\epsilon_c^2} + \sum_{r=1}^{N_{r'}} \frac{f_r}{\epsilon_r^2} + \frac{f_{e1}}{\epsilon_{e1}^2} + \frac{f_{e2}}{\epsilon_{e2}^2} \quad (13)$$

$$S^{(\ell)}(-3) = \sum_{c=1}^{N_c} \frac{f_c}{\epsilon_c^3} + \sum_{r=1}^{N_{r'}} \frac{f_r}{\epsilon_r^3} + \frac{f_{e1}}{\epsilon_{e1}^3} + \frac{f_{e2}}{\epsilon_{e2}^3}, \quad (14)$$

As an example, Fig. 1 depicts the dipole transitions included in the sum-rules for lithium. The core electrons were considered separately and assumed to only excite to a pseudo-state with an energy

$\Delta$  for each multipole. The resulting core oscillator distribution ( $f_c, \epsilon_c$ ) is discussed later. The valence excitations were described in two different ways as in Eq. 9 and Eq. 10.

**Fig. 1:** Schematic of the dipole transitions included in the sum-rules for lithium. The  $1s^2$  core electrons were assumed to only excite (via the dot-dashed line) to a  $1s2\tilde{p}$  pseudo-state with an energy  $\Delta$ . The valence excitations are shown in two different ways as per Eq. 9 and Eq. 10: (a) is the case of Eq. 9 where the primary transitions are shown with solid connecting lines, whilst a large number of dashed-lines to highly-excited bound states (up to  $np$ ) are included as well as pseudo-states (up to  $n\bar{p}$ ) to describe the excitations to the continuum. (b) is the case of Eq. 10 where the transitions to  $2p_J$  and  $3p_J$  states were still included while only three effective transitions (the dot-dashed lines to the  $np'$  states) are adopted to represent the contributions from excitations to the highly-excited bound states as well as the continuum states.

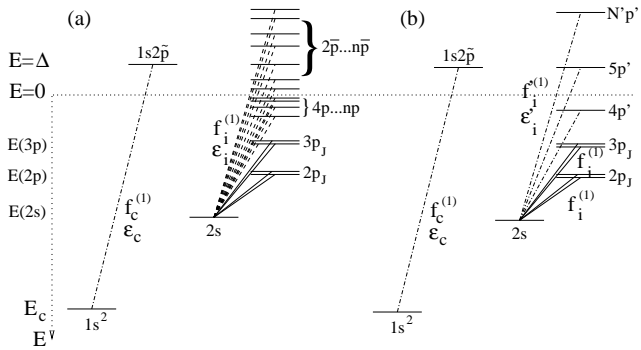


Table A shows the numerical convergence of the dispersion coefficients of lithium dimer calculated using effective oscillator strength distributions with varying sizes. The oscillator strengths of the lowest four physical transitions for dipole and octupole and lowest six physical transitions for quadrupole were included in the calculations and the number of effective oscillator strengths varied from  $N_e = 0$  to  $N_e = 3$ . The exact results were produced using Eq. 9. A reasonable assessment is that each additional effective oscillator strength increases the accuracy by two orders of magnitude. Almost all of the effective oscillator strength distributions used in this paper have three effective oscillator strengths. This is sufficient to achieve an overall accuracy of at least five significant digits in the dispersion parameters.

Since there are three effective oscillator strengths adopted for almost all of the systems in the present work, six sum-rules were used to build a set of six non-linear equations and obtain the effective oscillator strength distribution. The set of equations were solved with the Mathematica program which sometimes failed when the non-linear equations had a dimensionality of 6. In such cases, the energy of the third effective oscillator strength was fixed manually and the dimensionality of the non-linear equations was reduced to be 5. The energy of the third effective oscillator strength was adjusted manually until the non-linear equations gave correct solutions.

Table A

Convergence of the  $C_n$  dispersion parameters (in a.u.) for lithium dimer. The parameters are calculated using effective oscillator strength distributions with different sizes.  $N_e$  gives the number of effective oscillator strengths that were adopted. The ‘exact’ results were calculated using Eq. 9. We thus adopt the  $N_e = 3$  set of effective oscillator strengths, ie. for each multipole  $(f_{e1}^{(\ell)}, \varepsilon_{e1}^{(\ell)}, f_{e2}^{(\ell)}, \varepsilon_{e2}^{(\ell)}, f_{e3}^{(\ell)}, \varepsilon_{e3}^{(\ell)})$ , which are given later in the paper.

$N_e$	$C_6$	$10^{-4} \times C_8$	$10^{-6} \times C_{10}$
0	1351.144	7.190653	3.899799
1	1384.730	8.294263	7.294936
2	1395.684	8.353312	7.381506
3	1395.782	8.354554	7.382932
exact	1395.785	8.354584	7.382907

## 2.2. Casimir-Polder relations

The dynamic polarizability at real frequencies is defined as

$$\alpha^{(\ell)}(\omega) = \sum_i \frac{f_{0i}^{(\ell)}}{\epsilon_{0i}^2 - \omega^2}, \quad (15)$$

where a pole exists whenever the frequency is equal to a transition frequency. At purely imaginary frequencies one has

$$\alpha^{(\ell)}(i\omega) = \sum_i \frac{f_{0i}^{(\ell)}}{\epsilon_{0i}^2 + \omega^2}, \quad (16)$$

and there are no longer any poles.

The atom wall coefficient [11, 30] can be written as

$$C_3 = \frac{1}{4\pi} \int_0^\infty d\omega \alpha_A^{(1)}(i\omega). \quad (17)$$

The  $C_6$  parameter is defined [26, 9],

$$C_6 = \frac{3}{\pi} \int_0^\infty d\omega \alpha_A^{(1)}(i\omega) \alpha_B^{(1)}(i\omega), \quad (18)$$

while  $C_8$  is [26, 9]

$$C_8 = \frac{15}{2\pi} \int_0^\infty d\omega \alpha_A^{(2)}(i\omega) \alpha_B^{(1)}(i\omega) + \frac{15}{2\pi} \int_0^\infty d\omega \alpha_A^{(1)}(i\omega) \alpha_B^{(2)}(i\omega), \quad (19)$$

and  $C_{10}$  [26, 9] is

$$\begin{aligned} C_{10} &= \frac{14}{\pi} \int_0^\infty d\omega \alpha_A^{(1)}(i\omega) \alpha_B^{(3)}(i\omega) + \frac{14}{\pi} \int_0^\infty d\omega \alpha_A^{(3)}(i\omega) \alpha_B^{(1)}(i\omega) \\ &+ \frac{35}{\pi} \int_0^\infty d\omega \alpha_A^{(2)}(i\omega) \alpha_B^{(2)}(i\omega). \end{aligned} \quad (20)$$

### 2.3. Quadrature rules for Casimir-Polder integrations

The Casimir-Polder integrals are over the frequency range from zero to infinity. The integration mesh is constructed by mapping a Gauss-Legendre quadrature grid defined over the  $[0, 1]$  interval to the  $[0, \infty)$  interval using the transformation [34]

$$\omega = \frac{au}{(1-u)}. \quad (21)$$

Making this transformation leads to a set of weights and abscissa that constitute the quadrature rule. A uniform quadrature rule was adopted for the tabulation of the dynamic polarizabilities. A Gauss-Legendre rule was adopted with the scaling parameter,  $a = 1.0$ .

The accuracy of the quadrature rule was tested by performing the calculations on cesium. Values of  $C_3$ ,  $C_6$ ,  $C_8$  and  $C_{10}$  are calculated both directly from the oscillator strength sum-rules and from the Casimir-Polder integrals. Table B shows that an integration rule with 40 quadrature points is sufficient to give  $C_6$  accurate to at least 8 significant digits. The values of  $C_8$  and  $C_{10}$  are even more accurate. Our least accurate dispersion parameter was  $C_3$  which was precise to 5 significant digits. Comparison with the quadrature rules of Derevianko *et al.* (DPB) [17], which used the transformation  $\omega = 2 \tan(u\pi/2)$  [17] are also given. The DPB quadrature rules were not as precise as present quadrature rules, with a 50 point rule giving only six digits accuracy for  $C_6$ . All of the calculations given in Table B were done with the values computed to machine accuracy.

The dynamic polarizabilities tabulated later are thus all given using a 40-point Gauss-Legendre rule with the scaling parameter set to  $a = 1.0$ . For convenience example weights and abscissa for this rule are given in Table C to 7 significant figures, although we do use the full machine precision in our later calculations. The discussion of the effect that resulted from the use of the truncated values from all of the tables is postponed towards the end of the paper.

## 3. Atomic Models

The atomic models used to construct the oscillator strength distributions are discussed here. The static multipole polarizabilities and the atom-wall dispersion parameter,  $C_3$ , for all systems are given in Table 1. Comparisons with selected high accuracy calculations and/or experimental data are also incorporated in Table 1. These tabulations enable an initial assessment of the reliability of the atomic structure models for the dispersion coefficient calculations that are presented later.

Table B

Convergence of the atom-wall coefficient  $C_3$  of cesium and dispersion coefficients  $C_n$  for cesium dimer. The first ‘exact’ row was computed using the sums as per Eqs. (5-8) including the full set of cesium states from the large-basis calculation. The other rows are all computed using Casimir-Polder integrals. The number of Gauss-Legendre integration points is  $N$ . The results labeled DPB- $N$  were computed using the tan-based transformation formula [17]. Note that the present calculations are all performed in full (double) precision (ie. the tables of values given in Ref. [17] to six digits were not used). All of the data is presented in a.u..

$N$	$C_3$	$C_6$	$C_8$	$C_{10}$
exact	4.26007137597965	6732.75009597686	1003153.22405625	157922221.743034
20	4.26019424843126	6732.66789142124	1003130.29211934	157920452.587935
30	4.26002633795384	6732.74957771718	1003153.17110936	157922219.833385
40	4.26006536827215	6732.75009436665	1003153.22396368	157922221.740791
50	4.26008159786497	6732.75009594827	1003153.22405587	157922221.743012
60	4.26007761977941	6732.75009597067	1003153.22405620	157922221.743030
DPB-20	4.25538440902656	6696.52470846661	997816.300124684	157387242.062778
DPB-30	4.26016857779331	6734.98988627677	1003351.22246868	157933531.124752
DPB-40	4.26007587763244	6732.66175250520	1003148.54915587	157922091.763271
DPB-50	4.26007949747275	6732.75267008174	1003153.29168060	157922221.708063
DPB-60	4.26007402950242	6732.75004218043	1003153.22411277	157922221.785811

### 3.1. Hydrogen

The hydrogen atom was diagonalized in a basis of  $N = 15$  Laguerre type orbitals for each angular momentum symmetry. Such a basis can give dispersion coefficients to an accuracy of 13 – 14 digits [35]. The resulting oscillator strength distribution does not include finite mass or relativistic effects. These two effects tend to cancel each other.

### 3.2. Core oscillator strength distributions for multi-electron atoms

The alkali and alkaline-earth atoms have both core and valence electrons. The oscillator strengths for the core were determined by using oscillator strength sum-rules as constraints [36, 4], i.e. the sum-rules computed using the core oscillator strength distribution must be equal to a previous theoretical or experimental estimate of the multipole polarizabilities of the core [37]. Especially, for dipole transitions one can use the TRK sum-rule as another constraint besides the core polarizability.

The initial estimate of the multipole oscillator strength for each shell is [36, 4]:

$$f_i^{(\ell)} = \ell N_i \langle r_i^{2\ell-2} \rangle, \quad (22)$$

where  $\langle r_i^{2\ell-2} \rangle$  expectation value is computed using the Hartree-Fock (HF) wave function for the core

Table C

Example Casimir-Polder integral grid locations ( $\omega_i$ ) and weights ( $w_i$ ) for 40-point integration.

$i$	$\omega_i$	$w_i$	$i$	$\omega_i$	$w_i$
1	8.819222E-04	2.264628E-03	21	1.080673E+00	1.677693E-01
2	4.658481E-03	5.298162E-03	22	1.262659E+00	1.972075E-01
3	1.150079E-02	8.400470E-03	23	1.477386E+00	2.335615E-01
4	2.149386E-02	1.160621E-02	24	1.732809E+00	2.790254E-01
5	3.476135E-02	1.495651E-02	25	2.039486E+00	3.366805E-01
6	5.147009E-02	1.849662E-02	26	2.411684E+00	4.109452E-01
7	7.183462E-02	2.227705E-02	27	2.869039E+00	5.083035E-01
8	9.612331E-02	2.635515E-02	28	3.439188E+00	6.385265E-01
9	1.246661E-01	3.079702E-02	29	4.162008E+00	8.167931E-01
10	1.578642E-01	3.567994E-02	30	5.096756E+00	1.067531E+00
11	1.962032E-01	4.109535E-02	31	6.334558E+00	1.431716E+00
12	2.402686E-01	4.715266E-02	32	8.021430E+00	1.981583E+00
13	2.907663E-01	5.398426E-02	33	1.040330E+01	2.852384E+00
14	3.485487E-01	6.175187E-02	34	1.392086E+01	4.317079E+00
15	4.146481E-01	7.065504E-02	35	1.942876E+01	6.982043E+00
16	4.903195E-01	8.094246E-02	36	2.876758E+01	1.237761E+01
17	5.770978E-01	9.292713E-02	37	4.652492E+01	2.512244E+01
18	6.768710E-01	1.070072E-01	38	8.695055E+01	6.351091E+01
19	7.919797E-01	1.236948E-01	39	2.146622E+02	2.441386E+02
20	9.253495E-01	1.436561E-01	40	1.133887E+03	2.911630E+03

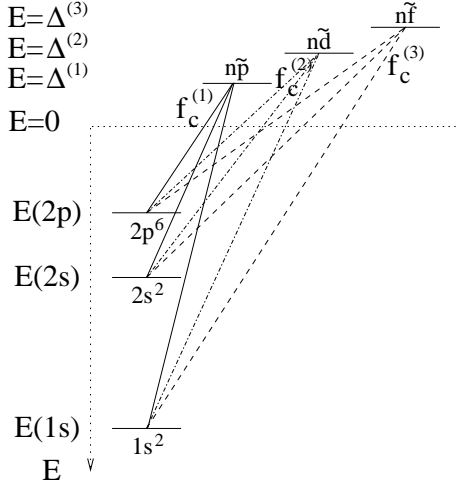
and  $N_i$  is the number of electrons in each shell. Obviously,  $f_i^{(\ell)}$  is equal to  $N_i$  for dipole transitions. Then an energy shift  $\Delta^{(\ell)}$  is applied to the Koopmans energy in order to make the core polarizabilities the same as the reference values for each multipole.

This technique can also be described as that all the core electrons are assumed to only excite to a pseudo-state with an energy of  $\Delta^{(\ell)}$  and the related oscillator strength is set by Eq. 22. As an example, Fig. 2 presents how we derived the dipole, quadrupole and octupole core oscillator strengths of Na. The core electrons were assumed to only excite to pseudo-states with energies  $\Delta^{(1)}$ ,  $\Delta^{(2)}$  and  $\Delta^{(3)}$  via dipole, quadrupole and octupole transitions respectively. The multipole oscillator strengths  $f_c^{(1)}$ ,  $f_c^{(2)}$  and  $f_c^{(3)}$  were set by Eq.22 and the energies  $\Delta^{(1)}$ ,  $\Delta^{(2)}$  and  $\Delta^{(3)}$  were solved with constraints that the sum-rules are equal to the reference values of the dipole, quadrupole and octupole polarizabilities.

### 3.3. General comment for the alkali atoms and alkali-like ions

The underlying structure models [38] used for the Li $\rightarrow$ Cs and Be $^+$  $\rightarrow$ Ba $^+$  sequences very closely resemble structure models used in previous non-relativistic calculations of these atoms [4]. Calculations

**Fig. 2:** Schematic of the dipole, quadrupole and octupole transitions to pseudo-states showing only the core excitations of Na. The  $1s^2 2s^2 2p^6$  core electrons are assumed to only excite to the pseudo-states  $n\tilde{p}$ ,  $n\tilde{d}$  and  $n\tilde{f}$  with energies  $\Delta^{(1)}$ ,  $\Delta^{(2)}$  and  $\Delta^{(3)}$  via dipole, quadrupole and octupole transitions respectively. The oscillator strengths are  $f_c^{(1)}$ ,  $f_c^{(2)}$  and  $f_c^{(3)}$  respectively.



are performed in a frozen core model, with the core taken from a Dirac-Fock calculation. A semi-empirical core polarization potential is used to incorporate the influence of core-valence correlations on the valence electron. The potential is adjusted so that the lowest energy of the state with a given  $(\ell, j)$  is the same as the experimental energy. The wave functions for the valence electrons are expanded in a basis of L-spinors [39, 38]. The impact of core-polarization upon the multipole transition operators are included when the transition matrix elements are computed [40]. The reduction of the calculation to effectively a one-electron problem makes it possible to eliminate basis set size as a significant source of error in the calculation.

For most of these atoms and ions, the binding energies of the lowest  $ns$ ,  $np_J$  and  $nd_J$  systems were tuned to be very close to experiment, typically the differences with experimental energies were less than  $10^{-6}$  Hartree. The energies of the next lowest excited states of each symmetry were not necessarily the same as experiment, but for the calculation of the dynamic polarizabilities these energies were adjusted manually to be the same as experiment.

### 3.4. Lithium

The present oscillator strength distributions are very similar to those used in a previous non-relativistic investigation of the dispersion coefficients of various low-lying states of the lithium dimer [41]. It can be seen from Table 1 that the present polarizabilities agree with Hylleraas calculations to an accuracy of about 0.1%.

### *3.5. Sodium*

As in the case for lithium, a previous non-relativistic investigation of the sodium polarizabilities and dispersion coefficients has been made with a structure model very similar with the present calculation [4, 42]. The differences in polarizabilities from this earlier calculation do not exceed 0.1%. Polarizabilities from the present calculation are within 0.5% of the polarizabilities from relativistic many-body perturbation theory calculations (RMBPT) [43, 17].

### *3.6. Potassium*

Details of the structure model can be found in previous works which investigated the tune-out wavelengths for potassium [38, 44]. Polarizabilities from this calculations are within 0.5% of the polarizabilities from RMBPT calculations [43, 17].

### *3.7. Rubidium*

The details of the model are very similar to a previous non-relativistic semi-empirical description of Rb [4]. Numerical values from this earlier calculation (labeled CICP) are included in Table 1 and are within 0.4% of the present polarizabilities. The polarizabilities from the RMBPT calculations [17] are all within 1% of the existing values.

### *3.8. Cesium*

The calculations on cesium are completely new and follow a methodology recently applied to other alkalis [38, 44]. The present and RMBPT polarizabilities agree to better than 1%.

### *3.9. Copper and Silver*

The models used for Cu and Ag were non-relativistic. The details of the model used to compute the oscillator strengths can be found in [45]. The core for these atoms contains a weakly bound  $(n - 1)d$  shell and the core polarizabilities are more than 10% of the total polarizability. The oscillator strength distribution does not allow for physical excitations out of the  $(n - 1)d$  core. The notional precision of the polarizabilities for these two atoms is about 5 – 10%.

### *3.10. Be<sup>+</sup>*

The polarizabilities of Be<sup>+</sup> have previously been computed with a non-relativistic semi-empirical model [46] and a Hylleraas calculation [47]. The present polarizabilities agree to better than 0.1% with the Hylleraas calculation.

### 3.11. $Mg^+$

The details of the present model are very similar to a previous non-relativistic semi-empirical description of  $Mg^+$  [48, 49]. The dipole polarizability of  $34.99\ a_0^3$  is very close to the experimental value of  $35.04(3)\ a_0^3$  [50, 49]. The higher order polarizabilities agree with RMBPT calculations at the 0.1% level.

### 3.12. $Ca^+$

The details of the calculation are very similar to a previous non-relativistic semi-empirical description of  $Ca^+$  [48]. All polarizabilities are in agreement with RMBPT calculations [51] to better than 1%.

### 3.13. $Sr^+$

The model used for  $Sr^+$  is relativistic. The details of the model are very similar to a previous non-relativistic semi-empirical description of  $Sr^+$  [52]. All polarizabilities are in agreement with RMBPT calculations to better than 1.5%.

### 3.14. $Ba^+$

The dipole and quadrupole polarizabilities are 2-3% smaller than RMBPT calculations [53, 54]. There is a large difference of the octupole. The  $\ell = 3$  orbitals are on the threshold of having an orbital collapse into an inner potential well [55, 56] and this makes the  $nf$  orbitals, and polarizabilities, relatively sensitive to very small changes in the interaction potential. So the 10% difference of the octupole with the RMBPT calculation was not surprising.

## 3.15. Beryllium

The Be transition matrix element list was obtained from a large dimension CI calculation with a semi-empirical polarization potential to represent core-valence correlations. The semi-empirical potential included both one and two body polarization potentials [4, 57]. For this calculation the energies of the lowest three dipole excited states were set to be the same as experiment [58]. These calculations are non-relativistic and hence do not explicitly include intercombination lines to the triplet states. Oscillator strengths for the transitions to the  ${}^3P_1^o$  states were added to the oscillator strength list by utilizing values from other atomic structure calculations [58, 59]. The intercombination transition has an insignificant affect on the dipole polarizability except at frequencies very close to the transition frequency. The level of agreement with calculations [60] that used explicitly correlated Gaussians (ECG) [61] is better than 0.2%. The ECG calculations did not include relativistic or finite mass effects.

### *3.16. Magnesium*

The structure calculations used to construct the oscillator strength distributions are described in Ref. [62]. The methodology is very similar to the approach adopted for beryllium. The energies of the three lowest  $^1P_1^o$  states were set to experimental values [63]. The level of agreement with fully relativistic configuration interaction plus many body perturbation theory calculations (RCI+MBPT) [13, 17] is better than 1% for the dipole and quadrupole polarizabilities with a 4% difference for the octupole polarizability. Oscillator strengths for the two lowest energy transitions to the  $^3P_1^o$  states were added to the oscillator strength list by utilizing values from other atomic structure calculations [58, 64, 65].

### *3.17. Calcium*

The structure calculations used to construct the oscillator strength distributions are described in Ref. [66]. The energies of the three lowest  $^1P_1^o$  states were set to experiment [63]. Oscillator strengths for the two lowest energy transitions to the  $^3P_1^o$  states were added to the oscillator strength list by utilizing matrix elements from other atomic structure calculations [58, 67]. The energies of the  $^3P_1^o$  state were set to experiment. The polarizabilities agree with RCI+MBPT calculations [13] to an accuracy of better than 1.5% for the dipole and quadrupole transitions. The level of agreement is poorer for the octupole polarizabilities with a discrepancy of 6%.

### *3.18. Strontium*

The structure calculations used to construct the oscillator strength distributions are described in Ref. [68]. The energies of the two lowest  $^1P_1^o$  states were set to be the same as experiment [63]. The matrix element for the resonant transition was set to experiment [68]. Oscillator strengths for the two lowest energy transitions to the  $^3P_1^o$  states were added to the oscillator strength list by utilizing values from other atomic structure calculations [58, 69]. The energies of the triplet state were set to experiment [63].

### *3.19. Barium*

The structure calculations for barium are new. These calculations follow the same non-relativistic technique used to determine wave functions and oscillator strengths for strontium [68]. The two electron binding energies of the lowest energy states were adjusted to be the same as experiment [63]. The matrix element for the resonant  $6s^2 \ ^1S_0^e - 6s6p \ ^1P_1^o$  transition was taken from experiment [70]. The oscillator strength for the intercombination line was added manually by utilizing a value from other atomic structure calculations [58, 71]. The energy of the triplet states were set to experiment.

### 3.20. Helium( $1s^2$ )

The helium wavefunctions were obtained using the configuration interaction (CI) method. The CI basis consisted of all possible configurations that could be formed from a single electron basis consisting of 30 Laguerre type orbitals [72] for each angular momentum with individual terms included up to  $\ell = 5$ . The parameter in the exponential term was set to 2.70. The polarizabilities agree to better than 0.05% with polarizabilities from Hylleraas calculations [11]. Omitted finite mass and relativistic effects are important at the 0.01% level of accuracy [73].

### 3.21. Neon, argon, krypton and xenon

The dipole oscillator strength distributions for rare gas atoms are those of Kumar and Meath [5, 6]. These distributions were derived from discrete transition rates and photoionization cross sections that were constrained to be consistent with the experimental refractive index and the Thomas-Reiche-Kuhn sum-rules. The accuracy assigned to the derived dispersion coefficients is typically of order 1%.

The method to determine the quadrupole and octupole oscillator strengths for the rare gas atoms is similar to the method described in section 3.2 for core excitations. A detailed description of the treatment can be found in [74]. A noteable difference with the determination of the core oscillator strength distribution is that one electron in the valence  $np$  shell is treated differently. This electron is assumed to excite to a pseudo-state with an energy  $\Delta_b^{(\ell)}$  while all of the other core electrons excite to a pseudo-state with an energy  $\Delta_a^{(\ell)}$ . The multipole oscillator strengths are also set by Eq.22 and the energies  $\Delta_a^{(\ell)}$  and  $\Delta_b^{(\ell)}$  are determined by constraining the oscillator strengths sum-rules to agree with sophisticated calculations of the multipole polarizabilities and the  $C_8$  and  $C_{10}$  coefficients for the homonuclear dimers [74, 75, 76, 77, 15].

In the case of Kr and Xe, corrections were made to the reference polarizabilities to incorporate relativistic effects. The accuracy of the quadrupole and octupole oscillator strength distributions has been estimated elsewhere [74]. A reasonable estimate of the relative uncertainty in any sum-rule utilizing the quadrupole or octupole dynamic polarizabilities would have 5% as the upper limit.

### 3.22. He( $1s2s\ ^3S^e$ )

The oscillator strength distribution used here was initially determined to compute the tune-out wavelengths of the helium metastable state [78]. The oscillator strength distribution was taken from a non-relativistic calculation computed within a frozen-core approximation in which the  $1s$  core electron could excite to three states. This was labeled as the CICP model [78].

### 3.23. Overview

The accuracy of the polarizabilities is system dependent. Results for the alkali atoms and alkali-like ions are generally the most accurate. The energies for the lowest dipole excited states are accurate to  $10^{-6}$  a.u.. The line strengths (i.e. the square of the reduced dipole matrix elements) are accurate to 0.1% for Li and  $\text{Be}^+$ . The accuracy degrades as the systems increase in size, and is probably about 1-2% for Cs and  $\text{Ba}^+$ .

The accuracy achieved for the alkaline-earth atoms is comparable in quality to that achieved for the corresponding alkali atom in the same row of the periodic table. Although the Hamiltonian is non-relativistic, the use of a tuned polarization potential to some extent compensates for relativistic effects. These can be seen from the comparisons between relativistic and non-relativistic polarizabilities of K using the present semi-empirical approach [79, 38]. The change in complexity going from one-electron atom to a two-electron atom hardly decreases the accuracy since the underlying configuration interaction calculations utilize very large basis with more than 150 orbitals.

The oscillator strength distributions for the alkali, and alkaline-earth ions will give reasonable descriptions of the actual dynamic dipole polarizabilities below the first two excitation thresholds. The dynamic polarizabilities for the alkaline-earth atoms will be reliable for energies below the excitation threshold for the resonant  $ns^2 \ ^1\text{D}^e \rightarrow nsnp \ ^1\text{P}^o$  transition. The dynamic polarizabilities for copper and silver should be reliable to the stated energies below the first excitation threshold. The oscillator strength distributions of rare gases can be expected to become less reliable as the first excitation threshold is reached.

## 4. Dynamic polarizability and dispersion coefficient tabulations

### 4.1. Real frequencies

The effective oscillator strength distributions for dipole, quadrupole and octupole transitions for all systems are given in Table 2. These distributions, by their design, give the same results as the large calculations shown in Table 1. They will also give reasonably accurate dynamic polarizabilities for real frequencies below the first excitation thresholds, although these are not presented here. Fortran programs that compute polarizabilities are available on a web-site maintained by the authors [80].

### 4.2. Imaginary frequencies

The dynamic polarizabilities for dipole, quadrupole and octupole transitions at imaginary energies are listed in Table 3. They are computed at frequencies based on a 40-point Gaussian rule that was used

for the consequent integrals presented in the paper. Note that the grids and integration weights used for the frequency integrations are given in Table C to 7 significant figures, although the calculations in Table 3 were performed at machine precision.

#### 4.3. Dispersion coefficients

Table 4 gives the  $C_6$ ,  $C_8$  and  $C_{10}$  dispersion coefficients for all combinations of the atoms listed in the article. This table was generated using the effective oscillator strength distributions (using full machine precision) using 40 point integrations. The  $C_6$  parameters in the tabulation lie very close to those of the Derevianko *et al.* tabulation [17] for systems involving the same atoms. The largest discrepancy for a homo-nuclear dimer occurs for barium and was 4%. The relative accuracy of the other dispersion coefficients can be estimated by reference to the text above and via the references where the initial versions of our oscillator strengths were first computed.

The long-range dispersion coefficients are also given for the ion-atom dimers, such as  $\text{Mg}^+ \text{-He}$ . The ion-atom interaction, however, also contains a (stronger) long-range polarization interaction. This has the form  $V \sim -\frac{1}{2}\alpha_d/R^4$  where  $\alpha_d$  is the static polarizability of the neutral atom [48].

Fortran programs that compute dispersion coefficients are available on a web-site maintained by the authors [80].

#### 4.4. Impact of finite precision tabulations

The final issue to consider here is the impact of using the tabulated values which are presented with less precision than were used in the actual calculations. As an example, reconsider the case of the dispersion coefficients of cesium as shown in Table B. With the 40-point integration rule the full machine precision calculations gave  $C_3 = 4.26006536827215$ ,  $C_6 = 6732.75009436665$ ,  $C_8 = 1003153.22396368$ ,  $C_{10} = 157922221.740791$ . If one uses the effective oscillator strengths as tabulated in Table B to compute the polarizabilities, at the frequencies tabulated in Table C, and then perform the integrations, then the result is  $C_3 = 4.2600653298881$ ,  $C_6 = 6732.74980359221$ ,  $C_8 = 1003153.18636727$ ,  $C_{10} = 157922216.822495$ . Thus the finite precision is not an issue since the noise generated by the truncation is much lower than the difference between the present dispersion coefficients and other accurate theoretical calculations.

### 5. Conclusion

Effective oscillator strength distributions and dynamic dipole polarizabilities at imaginary frequencies have been given for eighteen atoms and five alkali-like ions. All the atoms and ions are in a

spherically symmetric state. Providing the effective oscillator strength distributions means that the dynamic polarizabilities are not restricted to the frequencies tabulated here.

The present work should be regarded as the first step in an ongoing effort that aims to provide a data repository that will facilitate the determination of long-range interactions for more pairs of atomic and molecular systems [80].

## Acknowledgments

This research was supported by the Australian Research Council Discovery Project DP-1092620. The work of JJ was supported by the National Natural Science Foundation of China under Grant No. 11147018 and the basic scientific research foundation of institution of higher learning of Gansu Province. The work of YC was supported by the National Natural Science Foundation of China under Grant No. 11304063. MWJB was supported by the Australian Research Council Future Fellowship FT100100905, and thanks Julia M. Rossi for her work exploring the convergence of the Gaussian integration scheme that was used here.

This work is dedicated to Professor James (Jim) Mitroy, our colleague and mentor, who unexpectedly passed away shortly after the initial submission of this manuscript.

## References

- [1] R. Eisenschitz, F. London, *Z. Physik* 60 (1930) 491–527.
- [2] H. Margenau, *Rev. Mod. Phys.* 11 (1939) 1–35.
- [3] P. R. Fontana, *Phys. Rev.* 123 (1961) 1865.
- [4] J. Mitroy, M. W. J. Bromley, *Phys. Rev. A* 68 (2003) 052714.
- [5] A. Kumar, W. J. Meath, *Mol. Phys.* 54 (1985) 823.
- [6] A. Kumar, W. J. Meath, *Can. J. Chem.* 63 (1985) 1616.
- [7] H. B. Casimir, D. Polder, *Phys. Rev.* 73 (1948) 360–372.
- [8] M. Karplus, H. J. Kolker, *J. Chem. Phys.* 41 (1964) 3955–3961. doi:10.1063/1.1725842.
- [9] A. Koide, W. J. Meath, A. Allnatt, *J. Phys. Chem.* 86 (1982) 1222.
- [10] F. Maeder, W. Kutzelnigg, *Chem. Phys.* 42 (1979) 95.
- [11] Z. C. Yan, J. F. Babb, A. Dalgarno, G. W. F. Drake, *Phys. Rev. A* 54 (1996) 2824.
- [12] A. Derevianko, W. R. Johnson, M. S. Safronova, J. F. Babb, *Phys. Rev. Lett.* 82 (1999) 3589.

- [13] S. G. Porsev, A. Derevianko, *J. Exp. Theor. Phys.* 102 (2006) 195.
- [14] N. K. Rahman, A. Rizzo, D. L. Yeager, *Chem. Phys. Lett.* 166 (1990) 565–571. doi:10.1016/0009-2614(90)87152-H.
- [15] C. Hättig, B. A. Hess, *J. Chem. Phys.* 105 (1996) 9948–9965. doi:10.1063/1.472827.
- [16] A. Derevianko, J. F. Babb, A. Dalgarno, *Phys. Rev. A* 63 (2001) 052704.
- [17] A. Derevianko, S. G. Porsev, J. F. Babb, *At. Data Nucl. Data Tables* 96 (2010) 323–331.
- [18] C. Amiot, O. Dulieu, *J. Chem. Phys.* 117 (2002) 5155.
- [19] N. Vanhaecke, C. Lisdat, B. T'Jampens, D. Comparat, A. Crubellier, P. Pillet, *Eur. Phys. J. D* 28 (2004) 351.
- [20] V. V. Meshkov, A. V. Stolyariv, M. C. Heavan, C. Haugen, R. J. Le Roy, *J. Chem. Phys.* 140 (2014) 064315.
- [21] R. J. Le Roy, *Molec. Spectrosc. (Chem. Soc., London)* 1 (1973) 113.
- [22] B. Ji, C.-C. Tsai, W. C. Stwalley, *Chem. Phys. Lett.* 236 (1995) 242–246. doi:10.1016/0009-2614(95)00216-Q.
- [23] J. Mitroy, M. W. J. Bromley, *Phys. Rev. A* 68 (2003) 062710.
- [24] A. Dalgarno, *Adv. Chem. Phys.* 12 (1967) 143.
- [25] A. Dalgarno, *Rev. Mod. Phys.* 35 (1963) 522.
- [26] A. Dalgarno, W. D. Davison, *Adv. At. Mol. Phys.* 2 (1966) 1.
- [27] W. Kuhn, *Z. Phys.* 33 (1925) 408.
- [28] F. Reiche, W. Thomas, *Z. Phys.* 34 (1925) 510.
- [29] S. Wang, *Phys. Rev. A* 60 (1999) 262. doi:10.1103/PhysRevA.60.262.
- [30] P. Kharchenko, J. F. Babb, A. Dalgarno, *Phys. Rev. A* 55 (1997) 3566.
- [31] W. R. Johnson, V. A. Dzuba, U. I. Safronova, M. S. Safronova, *Phys. Rev. A* 69 (2004) 022508. doi:10.1103/PhysRevA.69.022508.
- [32] Y. H. Zhang, L. Y. Tang, X. Z. Zhang, J. Jiang, J. Mitroy, *J. Chem. Phys.* 136 (2012) 174107.
- [33] P. W. Langhoff, J. Sims, C. T. Corcoran, *Phys. Rev. A* 10 (1974) 829. doi:10.1103/PhysRevA.10.829.

- [34] J. M. Rossi, Atomic factorization of molecular interactions, Master's thesis, San Diego State University, 2011.
- [35] J. Mitroy, M. W. J. Bromley, Phys. Rev. A 71 (2005) 032709.
- [36] D. Rosenthal, R. P. McEachran, M. Cohen, Proc. R. Soc. London. Ser. A 337 (1974) 365.
- [37] J. Mitroy, M. W. J. Bromley, Phys. Rev. A 67 (2003) 034502.
- [38] J. Jiang, L. Y. Tang, J. Mitroy, Phys. Rev. A 87 (2013) 032518.
- [39] I. P. Grant, H. M. Quiney, Phys. Rev. A 62 (2000) 022508. doi:10.1103/PhysRevA.62.022508.
- [40] S. Hameed, A. Herzenberg, M. G. James, J. Phys. B 1 (1968) 822.
- [41] J. Y. Zhang, J. Mitroy, M. W. J. Bromley, Phys. Rev. A 75 (2007) 042509.
- [42] J. Mitroy, M. W. J. Bromley, Phys. Rev. A 71 (2005) 042701.
- [43] S. G. Porsev, A. Derevianko, J. Chem. Phys. 119 (2003) 844.
- [44] J. Jiang, J. Mitroy, Phys. Rev. A 88 (2013) 032505. doi:10.1103/PhysRevA.88.032505.
- [45] J. Y. Zhang, J. Mitroy, H. R. Sadeghpour, M. W. J. Bromley, Phys. Rev. A 78 (2008) 062710.
- [46] L.-Y. Tang, Z.-C. Yan, T.-Y. Shi, J. F. Babb, Phys. Rev. A 79 (2009) 062712.
- [47] L.-Y. Tang, Z.-C. Yan, T.-Y. Shi, J. Mitroy, Phys. Rev. A 81 (2010) 042521.
- [48] J. Mitroy, J. Y. Zhang, Eur. Phys. J D 46 (2008) 415.
- [49] J. Mitroy, M. S. Safronova, Phys. Rev. A 79 (2009) 012513.
- [50] E. L. Snow, S. R. Lundeen, Phys. Rev. A 77 (2008) 052501. doi:10.1103/PhysRevA.77.052501.
- [51] M. S. Safronova, U. I. Safronova, Phys. Rev. A 83 (2011) 012503. doi:10.1103/PhysRevA.83.012503.
- [52] J. Mitroy, J. Y. Zhang, M. W. J. Bromley, Phys. Rev. A 77 (2008) 032512.
- [53] E. Iskrenova-Tchoukova, M. S. Safronova, Phys. Rev. A 78 (2008) 012508. doi:10.1103/PhysRevA.78.012508.
- [54] U. I. Safronova, Phys. Rev. A 81 (2010) 052506. doi:10.1103/PhysRevA.81.052506.
- [55] T. B. Lucatorto, T. J. McIlrath, J. Sugar, S. M. Younger, Phys. Rev. Lett. 47 (1981) 1124–1128. doi:10.1103/PhysRevLett.47.1124.
- [56] K. T. Cheng, W. R. Johnson, Phys. Rev. A 28 (1983) 2820–2828. doi:10.1103/PhysRevA.28.2820.

- [57] J. Mitroy, Phys. Rev. A 82 (2010) 052516. doi:10.1103/PhysRevA.82.052516.
- [58] Y. Cheng, J. Jiang, J. Mitroy, Phys. Rev. A 88 (2013) 022511.
- [59] C. Froese Fischer, G. Tachiev, At. Data Nucl. Data Tables 87 (2004) 1.
- [60] J. Komasa, Phys. Rev. A 65 (2002) 012506.
- [61] J. Mitroy, S. Bubin, W. Horiuchi, Y. Suzuki, L. Adamowicz, W. Cencek, K. Szalewicz, J. Komasa, D. Blume, K. Varga, Rev. Mod. Phys. 85 (2013) 693–749. doi:10.1103/RevModPhys.85.693.
- [62] J. Mitroy, J. Y. Zhang, Mol. Phys. 106 (2008) 127.
- [63] A. Kramida, Y. Ralchenko, J. Reader, NIST ASD Team, NIST Atomic Spectra Database (version 5.0.0), 2012. URL: <http://physics.nist.gov/asd>.
- [64] C. Froese Fischer, G. Tachiev, A. Irimia, At. Data Nucl. Data Tables 92 (2006) 607.
- [65] C. F. Fischer, G. Tachiev, MCHF/MCDHF Collection, Version 2, Ref. No.13, 15 and 18, 2009. URL: <http://physics.nist.gov/mchf>.
- [66] J. Mitroy, J. Y. Zhang, J. Chem. Phys. 128 (2008) 134305.
- [67] C. F. Fischer, G. Tachiev, Phys. Rev. A. 68 (2003) 012507.
- [68] J. Mitroy, J. Y. Zhang, Mol. Phys. 108 (2010) 1999.
- [69] M. S. Safronova, S. G. Porsev, U. I. Safronova, M. G. Kozlov, C. W. Clark, Phys. Rev. A 87 (2013) 012509. doi:10.1103/PhysRevA.87.012509.
- [70] A. Bizzarri, M. C. E. Huber, Phys. Rev. A 42 (1990) 5422–5424. doi:10.1103/PhysRevA.42.5422.
- [71] V. A. Dzuba, J. S. M. Ginges, Phys. Rev. A 73 (2006) 032503.
- [72] M. W. J. Bromley, J. Mitroy, Phys. Rev. A 65 (2001) 012505.
- [73] K. Pachucki, J. Sapirstein, Phys. Rev. A 63 (2001) 012504. doi:10.1103/PhysRevA.63.012504.
- [74] J. Mitroy, J. Y. Zhang, Phys. Rev. A 76 (2007) 032706.
- [75] A. J. Thakkar, H. Hettema, P. E. S. Wormer, J. Chem. Phys. 97 (1992) 3252.
- [76] D. E. Woon, T. H. Dunning Jr, J. Chem. Phys. 100 (1994) 2975.
- [77] A. Nicklass, M. Dolg, H. Stoll, H. Preuss, J. Chem. Phys. 102 (1995) 8942.
- [78] J. Mitroy, L.-Y. Tang, Phys. Rev. A 88 (2013) 052515. doi:10.1103/PhysRevA.88.052515.
- [79] J. Mitroy, M. W. J. Bromley, Phys. Rev. A 71 (2005) 019902(E).

- [80] J. Mitroy, J. Jiang, Y. J. Cheng, M. W. J. Bromley, vdWwww dispersion interaction repository v2014.1, 2014. URL: <http://www.smp.uq.edu.au/people/brom/atomfoundry>.
- [81] Z.-C. Yan, J. F. Babb, Phys. Rev. A 58 (1998) 1247–1252. doi:10.1103/PhysRevA.58.1247.
- [82] Z. C. Yan, G. W. F. Drake, Phys. Rev. A 52 (1995) 3711.
- [83] P. Schwerdtfeger, G. A. Bowmaker, J. Chem. Phys. 100 (1994) 4487–4497. doi:10.1063/1.466280.
- [84] L.-Y. Tang, J.-Y. Zhang, Z.-C. Yan, T.-Y. Shi, J. F. Babb, J. Mitroy, Phys. Rev. A 80 (2009) 042511. doi:10.1103/PhysRevA.80.042511.
- [85] D. Jiang, B. Arora, M. S. Safranova, C. W. Clark, J. Phys. B 42 (2009) 154020.
- [86] B. Arora, D. K. Nandy, B. K. Sahoo, Phys. Rev. A 85 (2012) 012506. doi:10.1103/PhysRevA.85.012506.

## Explanation of Tables

**Table 1.** Multipole polarizabilities and atom-wall dispersion parameter for all atoms and ions.

The first row for any system is computed from the oscillator strength distributions used in this work. The other rows for each system give polarizabilities taken from other sources.

$C_3$	atom-wall dispersion parameter in a.u.
$\alpha_1$	static dipole polarizability in a.u.
$\alpha_2$	static quadrupole polarizability in a.u.
$\alpha_3$	static octupole polarizability in a.u.
Hyl	Hylleraas or correlated Slater basis
CICP	Configuration interaction with semi-empirical core-valence interaction
RMBPT	relativistic many-body perturbation theory
RCI+MBPT	relativistic configuration interaction with many-body perturbation theory to incorporate core-valence correlations. An asterisk is used to denote polarizabilities where the calculation matrix element for the resonance transition has been replaced by an experimental value.
ECG	explicitly correlated Gaussian basis
RCISD	relativistic configuration interaction calculations with single and double excitations.
RCCSD	relativistic coupled-cluster calculations and the contributions of singly and doubly excited states were considered.
Expt.	experimental value

**Table 2.** The dipole, quadrupole, and octupole effective oscillator strength distributions.

The oscillator strengths are in the  $f$  column and excitation energies (in a.u.) are given in the  $\varepsilon$  column. Effective oscillator strengths for alkali and alkaline-earth systems are given in the following order. Firstly the oscillator strengths for core excitations are given. These can be identified easily since the oscillator strength is usually a whole number, such as 2.0. Next, the oscillator strengths for physical transitions are listed. Finally, the effective oscillator strengths that account for transitions to the higher excited states and continuum are listed.

Different superscripts  $c$ ,  $r$ ,  $p$  and  $e$  are used to identify each transition corresponding to core excitations ( $c$ , computed as per [4]), real physical excitations ( $r$ ), excitations to pseudo-states ( $p$ ) and

effective excitations ( $e$ ). The calculations of the core for He( $1s2s\ ^3S^e$ ) adopted a different method that can be found in [78] and thus they are labeled by the superscript  $d$ . The oscillator strength distributions of the rare gas atoms are computed as per [5, 6, 74] and they are labeled by the superscript  $g$ .

$\ell$	the order of multipole
$\varepsilon$	excitation energy (in a.u.)
$f$	oscillator strength
Superscript $c$	core excitations
Superscript $r$	real physical excitations
Superscript $p$	excitaions to pseudo-states
Superscript $e$	effective excitations
Superscript $d$	core excitations for He( $1s2s\ ^3S^e$ )
Superscript $g$	rare gas atoms

**Table 3.** The dipole, quadrupole, and octupole dynamic polarizabilities of all atoms and ions (in a.u.).

The dynamic dipole, quadrupole, and octupole polarizabilities (in  $a_0^3$ ) at a set of photon energies that constitute a quadrature rule for the Casimir-Polder integral. The energies and integration weights are given in Table C.

**Table 4.** The dispersion coefficients,  $C_6$ ,  $C_8$  and  $C_{10}$  (in a.u.).

The dispersion coefficients,  $C_6$ ,  $C_8$  and  $C_{10}$  (in a.u.) for all possible pairs of atoms and ions. The He I(T) represents the He  $1s2s\ ^3S^e$ .

**Table 1**

Multipole static polarizabilities and atom-wall dispersion parameter for all atoms and ions. See Page 24 for explanation of tables.

System	$C_3$	$\alpha_1$	$\alpha_2$	$\alpha_3$
H	0.250	4.50	15.0	131.25
He	0.188132	1.38333	2.44596	10.6262
	0.188131 Hyl. [11]	1.38319 Hyl. [11]	2.44508 Hyl. [11]	10.6203 Hyl. [11]
He( $1s2s\ ^3S^e$ )	1.900	316.0	$2.708 \times 10^3$	$8.837 \times 10^4$
	1.90092 Hyl. [81]	315.63 Hyl. [81]	$2.7079 \times 10^3$ Hyl. [81]	$8.8377 \times 10^4$ Hyl. [81]
Li	1.524	164.3	$1.424 \times 10^3$	$3.968 \times 10^4$
	1.518001 Hyl. [82]	164.111 Hyl. [11]	$1.42327 \times 10^3$ Hyl. [11]	$3.96505 \times 10^4$ Hyl. [11]
	1.512 RMBPT [17]	164.0 RMBPT [17]	$1.424 \times 10^3$ RMBPT [43]	$3.957 \times 10^4$ RMBPT [43]
Be	1.010	37.73	300.4 [57]	$3.955 \times 10^3$ [57]
	1.01 RCI+MBPT [17]	37.76 RCI+MBPT [17]	300.6 RCI+MBPT [13]	$3.781 \times 10^3$ RCI+MBPT [13]
		37.755 ECG [60]	300.96 ECG [60]	
Ne	0.4751	2.669	7.518	42.07
	0.4751 Expt. [5]	2.669 Expt. [5]	7.518 MBPT [75]	42.07 MBPT [75]
Na	1.930	162.8	$1.878 \times 10^3$	$5.556 \times 10^4$
	1.871 RMBPT [17]	162.6 RMBPT [17]	$1.885 \times 10^3$ RMBPT [43]	$5.54 \times 10^4$ RMBPT [43]
Mg	1.704	71.37	811.4	$1.401 \times 10^4$
	1.666 RCI+MBPT [17]	71.26 RCI+MBPT [17]	812 RCI+MBPT [13]	$1.351 \times 10^4$ RCI+MBPT [13]
Ar	1.096	11.08	52.80	536.4 [74]
	1.096 Expt. [5]	11.08 Expt. [5]	51.86 MBPT [75]	536.4 MBPT [75]
K	3.018	290.0	$5.000 \times 10^3$	$1.775 \times 10^5$
	2.896 RMBPT [17]	290.2 RMBPT [17]	$5.000 \times 10^3$ RMBPT [43]	$1.77 \times 10^5$ RMBPT [43]
Ca	2.881	159.4	$3.082 \times 10^3$	$6.524 \times 10^4$ [66]
	2.744 RCI+MBPT [17]	157.1 RCI+MBPT* [17]	$3.081 \times 10^3$ RCI+MBPT [13]	$6.162 \times 10^4$ RCI+MBPT [13]
Cu	1.756	41.65	332.4	$5.580 \times 10^3$
		45.0 RCISD [83]		
Kr	1.542	16.79	98.20	$1.255 \times 10^3$ [74, 75, 15]
	1.542 Expt. [5]	16.79 Expt. [5]	99.30 MBPT [74]	$1.273 \times 10^3$ MBPT [75]
Rb	3.638	317.0	$6.479 \times 10^3$	$2.381 \times 10^5$ [4]
	3.426 RMBPT [17]	318.6 RMBPT [17]	$6.520 \times 10^4$ RMBPT [43]	$2.37 \times 10^5$ RMBPT [43]
	3.633 CICP [4]	315.7 CICP [4]	$6.480 \times 10^4$ CICP [4]	$2.378 \times 10^5$ CICP [4]
Sr	3.643	197.9	$4.643 \times 10^3$ [68]	$1.087 \times 10^5$ [68]
	3.382 RCI+MBPT [17]	197.2 RCI+MBPT* [17]	$4.630 \times 10^3$ RCI+MBPT [13]	$1.064 \times 10^5$ RCI+MBPT [13]
Ag	2.217	46.17	391.6	$7.194 \times 10^3$
		52.2 RCISD [83]		
Xe	2.164	27.16	213.7	$3.455 \times 10^3$ [74, 75]
	2.164 Expt. [5]	27.16 Expt. [5]	223.3 MBPT [74]	$3.646 \times 10^3$ [75]
Cs	4.260	396.7	$1.039 \times 10^4$	$3.972 \times 10^5$
	4.248 RMBPT [17]	399.8 RMBPT [17]	$1.047 \times 10^4$ RMBPT [43]	$3.95 \times 10^5$ RMBPT [43]
Ba	4.554	278.1	$8.789 \times 10^3$	$2.076 \times 10^5$
	4.294 RCI+MBPT [17]	273.5 RCI+MBPT [17]	$8.900 \times 10^3$ RCI+MBPT [13]	$2.060 \times 10^5$ RCI+MBPT [13]
Be <sup>+</sup>	0.5374	24.50	53.77	465.9
		24.489 Hyl. [47]	53.766 Hyl. [84]	465.76 Hyl. [84]
Mg <sup>+</sup>	0.9604	34.99	156.0	$1.715 \times 10^3$
		35.05 RMBPT [49]	156.1 RMBPT [49]	$1.719 \times 10^3$ RMBPT [49]
Ca <sup>+</sup>	1.746	75.46	874.5	$9.003 \times 10^3$
		76.1 RMBPT [51]	871 RMBPT [51]	$9.012 \times 10^3$ RMBPT [51]
Sr <sup>+</sup>	2.313	90.19	$1.356 \times 10^3$	$1.555 \times 10^4$
		91.3 RMBPT [85]	$1.366 \times 10^3$ RCCSD [86]	
Ba <sup>+</sup>	2.964	121.25	$4.071 \times 10^3$	$3.236 \times 10^4$
		124.15 RMBPT [53]	$4.182 \times 10^3$ RMBPT [53]	$3.647 \times 10^4$ RMBPT [54]



























**Table 3** (continued)

$i$	$\alpha_i^{(1)}$	$\alpha_i^{(2)}$	$\alpha_i^{(3)}$	$i$	$\alpha_i^{(1)}$	$\alpha_i^{(2)}$	$\alpha_i^{(3)}$
31	3.0635E-01	1.7618E+00	1.7774E+01	31	4.2206E-01	2.7586E+00	3.3520E+01
32	2.1502E-01	1.1287E+00	1.1207E+01	32	2.8719E-01	1.7669E+00	2.1076E+01
33	1.4426E-01	6.8687E-01	6.7158E+00	33	1.8550E-01	1.0746E+00	1.2607E+01
34	9.0574E-02	3.9119E-01	3.7717E+00	34	1.1262E-01	6.1156E-01	7.0717E+00
35	5.2038E-02	2.0392E-01	1.9436E+00	35	6.3774E-02	3.1884E-01	3.6414E+00
36	2.6780E-02	9.4023E-02	8.8859E-01	36	3.3469E-02	1.4731E-01	1.6641E+00
37	1.1919E-02	3.6206E-02	3.4016E-01	37	1.5800E-02	5.6938E-02	6.3692E-01
38	4.0550E-03	1.0417E-02	9.7448E-02	38	5.7792E-03	1.6430E-02	1.8245E-01
39	7.4403E-04	1.7141E-03	1.5992E-02	39	1.1062E-03	2.7070E-03	2.9942E-02
40	2.7504E-05	6.1486E-05	5.7318E-04	40	4.1197E-05	9.7159E-05	1.0732E-03

**Table 4**Dispersion coefficients of  $C_6$ ,  $C_8$  and  $C_{10}$ . See Page 25 for explanation of tables.

	$C_6$	$C_8$	$C_{10}$
H I - H I	6.4990E+00	1.2440E+02	3.2858E+03
H I - Li I	6.6591E+01	3.2824E+03	2.2318E+05
H I - Na I	7.4183E+01	4.0098E+03	2.9180E+05
H I - K I	1.1203E+02	7.9650E+03	7.3391E+05
H I - Rb I	1.2496E+02	9.5418E+03	9.3170E+05
H I - Cs I	1.4772E+02	1.2956E+04	1.4037E+06
H I - Cu I	3.8328E+01	1.3323E+03	5.5191E+04
H I - Ag I	4.5544E+01	1.6569E+03	6.9788E+04
H I - Be II	1.8835E+01	3.7173E+02	1.0203E+04
H I - Mg II	2.8792E+01	7.5290E+02	2.5138E+04
H I - Ca II	5.1768E+01	1.9598E+03	8.5616E+04
H I - Sr II	6.2806E+01	2.7013E+03	1.3012E+05
H I - Ba II	8.0740E+01	4.1196E+03	2.2737E+05
H I - Be I	3.4778E+01	1.2131E+03	4.6593E+04
H I - Mg I	5.7597E+01	2.5538E+03	1.2199E+05
H I - Ca I	1.0009E+02	6.3005E+03	4.0281E+05
H I - Sr I	1.1909E+02	8.4361E+03	6.0209E+05
H I - Ba I	1.5162E+02	1.2284E+04	9.9890E+05
H I - He I	2.8216E+00	4.1843E+01	8.7171E+02
H I - Ne I	5.6392E+00	9.7687E+01	2.2145E+03
H I - Ar I	1.9819E+01	4.4206E+02	1.2595E+04
H I - Kr I	2.8475E+01	7.1838E+02	2.3002E+04
H I - Xe I	4.2767E+01	1.3090E+03	4.9921E+04
H I - He I(T)	8.7865E+01	5.1854E+03	4.1782E+05
Li I - Li I	1.3958E+03	8.3546E+04	7.3828E+06
Li I - Na I	1.4729E+03	9.8851E+04	9.1880E+06
Li I - K I	2.3294E+03	1.9550E+05	2.1000E+07
Li I - Rb I	2.5428E+03	2.3323E+05	2.6114E+07
Li I - Cs I	3.0482E+03	3.1995E+05	3.8372E+07
Li I - Cu I	5.0563E+02	2.9652E+04	2.2788E+06
Li I - Ag I	5.7131E+02	3.4546E+04	2.7201E+06
Li I - Be II	2.8708E+02	1.2002E+04	7.7370E+05
Li I - Mg II	4.2236E+02	2.0472E+04	1.4079E+06
Li I - Ca II	8.2486E+02	5.0478E+04	3.6586E+06
Li I - Sr II	9.8172E+02	6.7264E+04	5.0651E+06
Li I - Ba II	1.2754E+03	1.0540E+05	8.0669E+06
Li I - Be I	4.7858E+02	2.7884E+04	2.0654E+06
Li I - Mg I	8.5714E+02	5.6764E+04	4.5353E+06
Li I - Ca I	1.6890E+03	1.4168E+05	1.2636E+07
Li I - Sr I	2.0386E+03	1.8988E+05	1.7901E+07
Li I - Ba I	2.6948E+03	2.8539E+05	2.8460E+07
Li I - He I	2.2535E+01	1.0842E+03	7.2665E+04
Li I - Ne I	4.3833E+01	2.2293E+03	1.5305E+05
Li I - Ar I	1.7413E+02	9.4947E+03	6.7817E+05
Li I - Kr I	2.5981E+02	1.4767E+04	1.0872E+06
Li I - Xe I	4.1103E+02	2.5213E+04	1.9576E+06
Li I - He I(T)	2.0924E+03	1.3261E+05	1.2805E+07
Na I - Na I	1.5616E+03	1.1582E+05	1.1335E+07
Na I - K I	2.4542E+03	2.2382E+05	2.5302E+07
Na I - Rb I	2.6814E+03	2.6505E+05	3.1263E+07
Na I - Cs I	3.2080E+03	3.5926E+05	4.5459E+07
Na I - Cu I	5.5290E+02	3.5549E+04	2.9050E+06
Na I - Ag I	6.2675E+02	4.1417E+04	3.4533E+06
Na I - Be II	3.1079E+02	1.4885E+04	1.0248E+06
Na I - Mg II	4.5879E+02	2.4988E+04	1.8361E+06
Na I - Ca II	8.8934E+02	5.9725E+04	4.6885E+06
Na I - Sr II	1.0593E+03	7.8696E+04	6.4345E+06
Na I - Ba II	1.3735E+03	1.2032E+05	1.0148E+07
Na I - Be I	5.2202E+02	3.3477E+04	2.6504E+06
Na I - Mg I	9.2994E+02	6.7237E+04	5.7357E+06
Na I - Ca I	1.8137E+03	1.6359E+05	1.5638E+07
Na I - Sr I	2.1855E+03	2.1720E+05	2.1948E+07
Na I - Ba I	2.8774E+03	3.2201E+05	3.4525E+07
Na I - He I	2.5759E+01	1.3269E+03	9.5213E+04
Na I - Ne I	5.0404E+01	2.7191E+03	1.9941E+05
Na I - Ar I	1.9679E+02	1.1520E+04	8.7726E+05
Na I - Kr I	2.9259E+02	1.7860E+04	1.3988E+06
Na I - Xe I	4.6079E+02	3.0314E+04	2.4962E+06

**Table 4** (continued)

	$C_6$	$C_8$	$C_{10}$
Na I - He I(T)	2.1792E+03	1.5526E+05	1.5700E+07
K I - K I	3.9063E+03	4.1947E+05	5.3694E+07
K I - Rb I	4.2683E+03	4.9099E+05	6.5417E+07
K I - Cs I	5.1239E+03	6.5703E+05	9.3230E+07
K I - Cu I	8.4796E+02	6.9141E+04	6.8927E+06
K I - Ag I	9.6113E+02	7.9950E+04	8.0944E+06
K I - Be II	4.7511E+02	3.1402E+04	2.7083E+06
K I - Mg II	6.9946E+02	5.0763E+04	4.6384E+06
K I - Ca II	1.3721E+03	1.1700E+05	1.1358E+07
K I - Sr II	1.6364E+03	1.5116E+05	1.5238E+07
K I - Ba II	2.1300E+03	2.2784E+05	2.3604E+07
K I - Be I	7.9182E+02	6.5121E+04	6.3773E+06
K I - Mg I	1.4176E+03	1.2814E+05	1.3324E+07
K I - Ca I	2.8036E+03	3.0290E+05	3.4660E+07
K I - Sr I	3.3900E+03	3.9717E+05	4.7656E+07
K I - Ba I	4.4922E+03	5.8401E+05	7.3555E+07
K I - He I	3.9468E+01	2.6207E+03	2.3966E+05
K I - Ne I	7.7456E+01	5.3056E+03	4.9325E+05
K I - Ar I	2.9937E+02	2.2265E+04	2.1304E+06
K I - Kr I	4.4419E+02	3.4291E+04	3.3494E+06
K I - Xe I	6.9807E+02	5.7478E+04	5.8324E+06
K I - He I(T)	3.5267E+03	3.0552E+05	3.4841E+07
Rb I - Rb I	4.6669E+03	5.7202E+05	7.9366E+07
Rb I - Cs I	5.6020E+03	7.6048E+05	1.1242E+08
Rb I - Cu I	9.3746E+02	8.2349E+04	8.6446E+06
Rb I - Ag I	1.0648E+03	9.5141E+04	1.0126E+07
Rb I - Be II	5.2176E+02	3.8105E+04	3.4780E+06
Rb I - Mg II	7.6914E+02	6.1048E+04	5.8985E+06
Rb I - Ca II	1.5065E+03	1.3896E+05	1.4315E+07
Rb I - Sr II	1.7983E+03	1.7840E+05	1.9101E+07
Rb I - Ba II	2.3408E+03	2.6626E+05	2.9494E+07
Rb I - Be I	8.7204E+02	7.7482E+04	8.0203E+06
Rb I - Mg I	1.5577E+03	1.5148E+05	1.6620E+07
Rb I - Ca I	3.0725E+03	3.5396E+05	4.2733E+07
Rb I - Sr I	3.7150E+03	4.6178E+05	5.8440E+07
Rb I - Ba I	4.9205E+03	6.7505E+05	8.9750E+07
Rb I - He I	4.4785E+01	3.1449E+03	3.0435E+05
Rb I - Ne I	8.8181E+01	6.3556E+03	6.2428E+05
Rb I - Ar I	3.3723E+02	2.6567E+04	2.6855E+06
Rb I - Kr I	4.9916E+02	4.0841E+04	4.2096E+06
Rb I - Xe I	7.8197E+02	6.8221E+04	7.2918E+06
Rb I - He I(T)	3.8470E+03	3.6394E+05	4.3003E+07
Cs I - Cs I	6.7328E+03	1.0032E+06	1.5792E+08
Cs I - Cu I	1.1116E+03	1.1128E+05	1.2805E+07
Cs I - Ag I	1.2619E+03	1.2804E+05	1.4932E+07
Cs I - Be II	6.1989E+02	5.3027E+04	5.3539E+06
Cs I - Mg II	9.1303E+02	8.3780E+04	8.9340E+06
Cs I - Ca II	1.7922E+03	1.8830E+05	2.1402E+07
Cs I - Sr II	2.1394E+03	2.3971E+05	2.8321E+07
Cs I - Ba II	2.7874E+03	3.5444E+05	4.3650E+07
Cs I - Be I	1.0343E+03	1.0448E+05	1.1923E+07
Cs I - Mg I	1.8496E+03	2.0281E+05	2.4404E+07
Cs I - Ca I	3.6592E+03	4.6858E+05	6.1727E+07
Cs I - Sr I	4.4276E+03	6.0764E+05	8.3763E+07
Cs I - Ba I	5.8743E+03	8.8363E+05	1.2792E+08
Cs I - He I	5.2679E+01	4.2731E+03	4.5827E+05
Cs I - Ne I	1.0361E+02	8.5934E+03	9.3456E+05
Cs I - Ar I	3.9759E+02	3.5712E+04	3.9953E+06
Cs I - Kr I	5.8892E+02	5.4728E+04	6.2334E+06
Cs I - Xe I	9.2334E+02	9.0918E+04	1.0705E+07
Cs I - He I(T)	4.6444E+03	5.0133E+05	6.2588E+07
Cu I - Cu I	2.4956E+02	1.1966E+04	6.6737E+05
Cu I - Ag I	2.9161E+02	1.4621E+04	8.2140E+05
Cu I - Be II	1.2667E+02	4.2351E+03	1.7686E+05
Cu I - Mg II	1.9170E+02	7.6072E+03	3.6183E+05
Cu I - Ca II	3.5636E+02	1.8379E+04	1.0366E+06
Cu I - Sr II	4.2976E+02	2.4663E+04	1.4918E+06
Cu I - Ba II	5.5360E+02	3.7146E+04	2.4563E+06
Cu I - Be I	2.2494E+02	1.1008E+04	5.8993E+05

**Table 4** (continued)

	$C_6$	$C_8$	$C_{10}$
Cu I - Mg I	3.8423E+02	2.2203E+04	1.3793E+06
Cu I - Ca I	7.0110E+02	5.3305E+04	4.0761E+06
Cu I - Sr I	8.3910E+02	7.0819E+04	5.8899E+06
Cu I - Ba I	1.0820E+03	1.0332E+05	9.4792E+06
Cu I - He I	1.6253E+01	4.7707E+02	1.7184E+04
Cu I - Ne I	3.2893E+01	1.0296E+03	3.8818E+04
Cu I - Ar I	1.1440E+02	4.2911E+03	1.8638E+05
Cu I - Kr I	1.6531E+02	6.6920E+03	3.1270E+05
Cu I - Xe I	2.5076E+02	1.1493E+04	6.0348E+05
Cu I - He I(T)	6.9860E+02	4.6172E+04	4.0660E+06
Ag I - Ag I	3.4229E+02	1.7945E+04	1.0281E+06
Ag I - Be II	1.4581E+02	5.1026E+03	2.2315E+05
Ag I - Mg II	2.2125E+02	9.1576E+03	4.5006E+05
Ag I - Ca II	4.0998E+02	2.1821E+04	1.2648E+06
Ag I - Sr II	4.9558E+02	2.9220E+04	1.8099E+06
Ag I - Ba II	6.3859E+02	4.3681E+04	2.9578E+06
Ag I - Be I	2.6067E+02	1.3153E+04	7.2731E+05
Ag I - Mg I	4.4280E+02	2.6284E+04	1.6760E+06
Ag I - Ca I	8.0259E+02	6.2230E+04	4.8668E+06
Ag I - Sr I	9.6048E+02	8.2414E+04	6.9949E+06
Ag I - Ba I	1.2367E+03	1.1962E+05	1.1188E+07
Ag I - He I	1.9754E+01	6.4142E+02	2.2027E+04
Ag I - Ne I	4.0040E+01	1.4043E+03	5.0185E+04
Ag I - Ar I	1.3790E+02	5.5001E+03	2.3851E+05
Ag I - Kr I	1.9859E+02	8.4842E+03	3.9791E+05
Ag I - Xe I	2.9979E+02	1.4370E+04	7.6086E+05
Ag I - He I(T)	7.8539E+02	5.3449E+04	4.8090E+06
Be II - Be II	6.8796E+01	1.1536E+03	3.1769E+04
Be II - Mg II	1.0297E+02	2.3959E+03	7.8350E+04
Be II - Ca II	1.9188E+02	6.9308E+03	2.7497E+05
Be II - Sr II	2.2931E+02	9.7767E+03	4.2384E+05
Be II - Ba II	2.9501E+02	1.5672E+04	7.5852E+05
Be II - Be I	1.2024E+02	3.8803E+03	1.4602E+05
Be II - Mg I	2.0800E+02	8.5937E+03	3.9346E+05
Be II - Ca I	3.8460E+02	2.3208E+04	1.3693E+06
Be II - Sr I	4.5953E+02	3.1852E+04	2.0877E+06
Be II - Ba I	5.9416E+02	4.8107E+04	3.5612E+06
Be II - He I	6.9817E+00	1.2046E+02	2.7661E+03
Be II - Ne I	1.3709E+01	2.7401E+02	6.8468E+03
Be II - Ar I	5.2100E+01	1.2531E+03	3.8038E+04
Be II - Kr I	7.6651E+01	2.0411E+03	6.9164E+04
Be II - Xe I	1.1890E+02	3.7509E+03	1.4909E+05
Be II - He I(T)	4.0061E+02	1.9760E+04	1.4991E+06
Mg II - Mg II	1.5459E+02	4.6006E+03	1.7633E+05
Mg II - Ca II	2.8682E+02	1.2152E+04	5.6242E+05
Mg II - Sr II	3.4321E+02	1.6728E+04	8.4024E+05
Mg II - Ba II	4.4120E+02	2.5977E+04	1.4471E+06
Mg II - Be I	1.8090E+02	7.0269E+03	3.0869E+05
Mg II - Mg I	3.1181E+02	1.4917E+04	7.7794E+05
Mg II - Ca I	5.7274E+02	3.8201E+04	2.5160E+06
Mg II - Sr I	6.8388E+02	5.1663E+04	3.7466E+06
Mg II - Ba I	8.8234E+02	7.6758E+04	6.2299E+06
Mg II - He I	1.0909E+01	2.5265E+02	7.4807E+03
Mg II - Ne I	2.1572E+01	5.5418E+02	1.7525E+04
Mg II - Ar I	8.0615E+01	2.4362E+03	8.8909E+04
Mg II - Kr I	1.1829E+02	3.8861E+03	1.5453E+05
Mg II - Xe I	1.8287E+02	6.9169E+03	3.1411E+05
Mg II - He I(T)	5.8526E+02	3.2851E+04	2.6337E+06
Ca II - Ca II	5.4103E+02	2.9991E+04	1.6728E+06
Ca II - Sr II	6.4740E+02	4.0084E+04	2.4249E+06
Ca II - Ba II	8.3500E+02	6.1023E+04	4.1083E+06
Ca II - Be I	3.3247E+02	1.7066E+04	9.1360E+05
Ca II - Mg I	5.7872E+02	3.4964E+04	2.1610E+06
Ca II - Ca I	1.0850E+03	8.6387E+04	6.5768E+06
Ca II - Sr I	1.3004E+03	1.1527E+05	9.5769E+06
Ca II - Ba I	1.6895E+03	1.7012E+05	1.5644E+07
Ca II - He I	1.9724E+01	6.5887E+02	2.7083E+04
Ca II - Ne I	3.9136E+01	1.3958E+03	6.0177E+04
Ca II - Ar I	1.4507E+02	5.9659E+03	2.8288E+05

**Table 4** (continued)

	$C_6$	$C_8$	$C_{10}$
Ca II - Kr I	2.1277E+02	9.3534E+03	4.7088E+05
Ca II - Xe I	3.2907E+02	1.6181E+04	8.9996E+05
Ca II - He I(T)	1.1692E+03	8.0255E+04	6.6137E+06
Sr II - Sr II	7.7572E+02	5.2944E+04	3.4731E+06
Sr II - Ba II	1.0010E+03	7.9486E+04	5.8177E+06
Sr II - Be I	3.9816E+02	2.2920E+04	1.3292E+06
Sr II - Mg I	6.9181E+02	4.6238E+04	3.0709E+06
Sr II - Ca I	1.2953E+03	1.1175E+05	9.0927E+06
Sr II - Sr I	1.5531E+03	1.4793E+05	1.3105E+07
Sr II - Ba I	2.0179E+03	2.1663E+05	2.1191E+07
Sr II - He I	2.4404E+01	9.1341E+02	4.1735E+04
Sr II - Ne I	4.8613E+01	1.9200E+03	9.1490E+04
Sr II - Ar I	1.7802E+02	8.1177E+03	4.2158E+05
Sr II - Kr I	2.6040E+02	1.2655E+04	6.9326E+05
Sr II - Xe I	4.0131E+02	2.1682E+04	1.3007E+06
Sr II - He I(T)	1.3920E+03	1.0610E+05	9.0037E+06
Ba II - Ba II	1.2932E+03	1.1794E+05	1.0092E+07
Ba II - Be I	5.1133E+02	3.4369E+04	2.2131E+06
Ba II - Mg I	8.8932E+02	6.8506E+04	4.9845E+06
Ba II - Ca I	1.6714E+03	1.6342E+05	1.4457E+07
Ba II - Sr I	2.0062E+03	2.1474E+05	2.0670E+07
Ba II - Ba I	2.6116E+03	3.1323E+05	3.3529E+07
Ba II - He I	3.1504E+01	1.3969E+03	7.3918E+04
Ba II - Ne I	6.2753E+01	2.9052E+03	1.5938E+05
Ba II - Ar I	2.2944E+02	1.2141E+04	7.1777E+05
Ba II - Kr I	3.3537E+02	1.8809E+04	1.1637E+06
Ba II - Xe I	5.1640E+02	3.1891E+04	2.1351E+06
Ba II - He I(T)	1.8209E+03	1.7008E+05	1.4125E+07
Be I - Be I	2.1341E+02	1.0213E+04	5.1558E+05
Be I - Mg I	3.6489E+02	2.0785E+04	1.2298E+06
Be I - Ca I	6.6161E+02	5.0167E+04	3.7170E+06
Be I - Sr I	7.8846E+02	6.6676E+04	5.4074E+06
Be I - Ba I	1.0136E+03	9.7059E+04	8.7571E+06
Be I - He I	1.3228E+01	4.2473E+02	1.4564E+04
Be I - Ne I	2.6000E+01	9.0423E+02	3.3184E+04
Be I - Ar I	9.7824E+01	3.8172E+03	1.5970E+05
Be I - Kr I	1.4332E+02	5.9702E+03	2.6957E+05
Be I - Xe I	2.2099E+02	1.0309E+04	5.2553E+05
Be I - He I(T)	6.5535E+02	4.3495E+04	3.7257E+06
Mg I - Mg I	6.2959E+02	4.1514E+04	2.8090E+06
Mg I - Ca I	1.1580E+03	9.8132E+04	8.0893E+06
Mg I - Sr I	1.3825E+03	1.2941E+05	1.1570E+07
Mg I - Ba I	1.7843E+03	1.8747E+05	1.8428E+07
Mg I - He I	2.1452E+01	8.8409E+02	3.9341E+04
Mg I - Ne I	4.2182E+01	1.8439E+03	8.6403E+04
Mg I - Ar I	1.5979E+02	7.7228E+03	3.9748E+05
Mg I - Kr I	2.3494E+02	1.1978E+04	6.5325E+05
Mg I - Xe I	3.6412E+02	2.0384E+04	1.2238E+06
Mg I - He I(T)	1.1893E+03	8.7668E+04	7.9675E+06
Ca I - Ca I	2.1882E+03	2.2674E+05	2.2084E+07
Ca I - Sr I	2.6237E+03	2.9567E+05	3.0927E+07
Ca I - Ba I	3.4168E+03	4.2630E+05	4.8387E+07
Ca I - He I	3.6597E+01	2.1397E+03	1.3217E+05
Ca I - Ne I	7.1985E+01	4.3683E+03	2.8024E+05
Ca I - Ar I	2.7403E+02	1.8149E+04	1.2389E+06
Ca I - Kr I	4.0419E+02	2.7911E+04	1.9830E+06
Ca I - Xe I	6.2959E+02	4.6746E+04	3.5614E+06
Ca I - He I(T)	2.4120E+03	2.1796E+05	2.1475E+07
Sr I - Sr I	3.1493E+03	3.8352E+05	4.2947E+07
Sr I - Ba I	4.1086E+03	5.5065E+05	6.6687E+07
Sr I - He I	4.3813E+01	2.8557E+03	1.9831E+05
Sr I - Ne I	8.6359E+01	5.8012E+03	4.1634E+05
Sr I - Ar I	3.2707E+02	2.4019E+04	1.8200E+06
Sr I - Kr I	4.8206E+02	3.6844E+04	2.8908E+06
Sr I - Xe I	7.5031E+02	6.1402E+04	5.1257E+06
Sr I - He I(T)	2.9290E+03	2.9164E+05	3.0025E+07
Ba I - Ba I	5.3796E+03	7.8975E+05	1.0323E+08
Ba I - He I	5.5602E+01	4.1341E+03	3.2920E+05
Ba I - Ne I	1.0957E+02	8.3524E+03	6.8399E+05

**Table 4** (continued)

	$C_6$	$C_8$	$C_{10}$
Ba I - Ar I	4.1547E+02	3.4488E+04	2.9596E+06
Ba I - Kr I	6.1267E+02	5.2783E+04	4.6659E+06
Ba I - Xe I	9.5441E+02	8.7578E+04	8.1673E+06
Ba I - He I(T)	3.9209E+03	4.4297E+05	4.7194E+07
He I - He I	1.4612E+00	1.4123E+01	1.8379E+02
He I - Ne I	3.0319E+00	3.6219E+01	5.4452E+02
He I - Ar I	9.5519E+00	1.6757E+02	3.7093E+03
He I - Kr I	1.3417E+01	2.7621E+02	7.1661E+03
He I - Xe I	1.9575E+01	5.1022E+02	1.6580E+04
He I - He I(T)	2.9078E+01	1.7005E+03	1.3638E+05
Ne I - Ne I	6.3826E+00	9.0265E+01	1.5328E+03
Ne I - Ar I	1.9502E+01	3.8891E+02	9.3345E+03
Ne I - Kr I	2.7300E+01	6.2738E+02	1.7396E+04
Ne I - Xe I	3.9661E+01	1.1276E+03	3.8565E+04
Ne I - He I(T)	5.6444E+01	3.4585E+03	2.8318E+05
Ar I - Ar I	6.4300E+01	1.6215E+03	4.9033E+04
Ar I - Kr I	9.1126E+01	2.5711E+03	8.6774E+04
Ar I - Xe I	1.3446E+02	4.5267E+03	1.8074E+05
Ar I - He I(T)	2.2655E+02	1.4654E+04	1.2354E+06
Kr I - Kr I	1.2956E+02	4.0400E+03	1.5013E+05
Kr I - Xe I	1.9193E+02	7.0260E+03	3.0346E+05
Kr I - He I(T)	3.3922E+02	2.2686E+04	1.9579E+06
Xe I - Xe I	2.8587E+02	1.2004E+04	5.8821E+05
Xe I - He I(T)	5.3940E+02	3.8407E+04	3.4571E+06
He I(T) - He I(T)	3.2825E+03	2.1070E+05	2.1792E+07